6-1-2003

Chromatin of endoreduplicated pavement cells has greater range of movement than that of diploid guard cells in Arabidopsis thaliana

Naohiro Kato
Rutgers University–New Brunswick

Eric Lam
Rutgers University–New Brunswick

Recommended Citation

Kato, N., & Lam, E. (2003). Chromatin of endoreduplicated pavement cells has greater range of movement than that of diploid guard cells in Arabidopsis thaliana. *Journal of Cell Science, 116* (11), 2195-2201. https://doi.org/10.1242/jcs.00437

Chromatin of endoreduplicated pavement cells has greater range of movement than that of diploid guard cells in *Arabidopsis thaliana*

Naohiro Kato and Eric Lam*

Biotech Center for Agriculture and The Environment, Rutgers The State University of New Jersey, New Brunswick, NJ 08901, USA
*Author for correspondence (e-mail: lam@aesop.rutgers.edu)

Accepted 21 February 2003
Journal of Cell Science 116, 2195-2201 © 2003 The Company of Biologists Ltd
doi:10.1242/jcs.00437

Summary

In the current model of chromatin organization in the interphase cell nucleus, chromosomes are organized into territories. Although constrained diffusion of chromatin in interphase cells has been confirmed in all cell types examined, little is known about chromatin dynamics in plant interphase cells. In this work, we measured for the first time interphase chromatin dynamics in plants using the green-fluorescent-protein-mediated chromatin-tagging system. Moreover, we compared the dynamics of diploid guard cells and endoreduplicated pavement cells. The movement of tagged loci in live seedlings shows constrained behavior in both types of nuclei. However, we found that the apparent confinement area for tagged loci in pavement cells is over 6 times larger than it is in guard cells. These findings suggest that chromatin is anchored to some component of the nucleus and that this might be responsible for the different dynamics of chromatin diffusion between diploid cells and endoreduplicated cells.

Key words: Endoreduplication, Polyploidy, Chromatin dynamics, GFP, *Arabidopsis*

Introduction

Fluorescence in situ hybridization analysis has shown that chromatin in eukaryote interphase cells including plants are fairly well organized (Cremer and Cremer, 2001; Fransz et al., 2002; Lysak et al., 2001). Studies using the *lac*-repressor (LacI)/green-fluorescent-protein (GFP) + *lac*-operator tagging system in budding yeast (Heun et al., 2001; Marshall et al., 1997a), dissected *Drosophila* tissues (Marshall et al., 1997a; Vazquez et al., 2001) and cultured mammalian cells (Chubb et al., 2002) showed that chromatin dynamics in interphase nuclei are generally constrained. This implies that chromosomes are anchored within the nucleus, at such sites as nuclear pores or nuclear lamina in fungi and animal cells (Chubb et al., 2002; Heun et al., 2001; Ishii et al., 2002). Chromatin dynamics in plant interphase cells has been poorly characterized in comparison.

We previously demonstrated the feasibility of detecting and tracking specific insertion sites in live *Arabidopsis* plants with the LacI-GFP + *lac*-operator tagging system (Kato and Lam, 2001). In this approach, concatameric arrays of *lac* operators (256-mer, 10.1 kbp) were randomly inserted into chromosomes along with a glucocorticoid-inducible system that drives expression of a fusion protein that consists of GFP, LacI DNA-binding domain and the SV40 T-antigen nuclear localization signal (GFP-LacI/NLS; Fig. 1a). Upon induction of GFP-LacI/NLS protein, we can detect the tagged loci as GFP-binding fluorescent spots. We showed that addition of isopropyl-β-D-1-thiogalactopyranoside (IPTG), which inhibits LacI binding to the *lac* operator, significantly decreased the number of detectable GFP spots. We also showed that the induced GFP-LacI/NLS fusion proteins do not localize to specific sites when the *lac* operator array is absent from the genome. These controls demonstrated that there are few artefacts in our system, in which 1-2-week-old seedlings with a size range of 5-10 mm are directly mounted on microscope slides with water as the mounting medium (Fig. 2a). Under these conditions, *Arabidopsis* seedlings can remain viable for at least 24 hours and can grow normally upon their return to soil.

In this work, we measured chromatin dynamics in interphase plant cells. This is the first report of such studies for live plants, to our knowledge. Moreover, we tested whether chromatin dynamics change in different cell types. In *Drosophila*, the confinement area of spermatocyte nuclei (Vazquez et al., 2001) is much larger than that of stage 12 embryos (Marshall et al., 1997b). However, it is not known whether these differences are a reflection of cell type or the GFP-tagged loci examined. In this work, we compared chromatin dynamics of specific loci in different cell types of the same transgenic plants so that we can eliminate locus- and sample-related variations. We chose to compare guard cells and pavement cells for two reasons. First, the two cell types are both located on the epidermis of the seedlings and can be distinguished by their shapes (Fig. 2b). Therefore, we could observe the nuclei of these cells with minimal optical perturbation. Second, most, if not all, the guard cells are diploid whereas most pavement cells are polyploid owing to DNA endoreduplication (Melaragno et al., 1993). Therefore, we might be able to correlate the effects of endoreduplication with changes in chromatin dynamics.

Endoreduplication is a phenomenon in which chromosomes duplicate without any obvious condensation and decondensation steps, leading to the production of

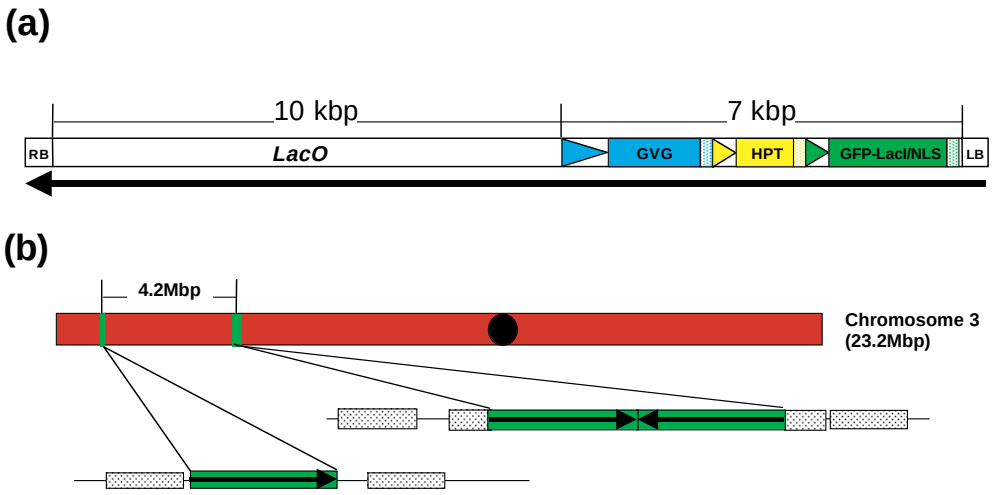

Fig. 1. Detailed genomic structure characterization of the T-DNA inserts in transgenic *Arabidopsis thaliana* line EL702C. (a) Schematic construct map of the T-DNA region in the binary vector pEL702. The plasmid was designed such that the DNA between the right and left borders (T-DNA) can be transferred into plant nuclei via *Agrobacterium*. Thus, when stable transgenic *Arabidopsis* plants are treated with the synthetic glucocorticoid dexamethasone (Dex), the expressed fusion proteins can localize to the integrated loci by association with the *lac* operator array. The numbers on the top indicate the size of DNA construct in kbp. The arrow indicates the orientation of T-DNA from the left border to right border. Colored areas indicate gene expression cassette: blue, glucocorticoid receptor expression; yellow, hygromycin phosphotransferase expression; green, GFP-LacI/NLS induced expression. Abbreviations and symbols: blue dot rectangle, pea rbcS-E9 terminator; blue triangle, cauliflower mosaic virus 35S promoter; green dot rectangle, pea rbcS-3A terminator; green rectangle, 6XGal4 UAS and TATA box; yellow dot rectangle, nopaline-synthase gene terminator; yellow triangle, nopaline-synthase gene promoter; GVG, glucocorticoid binding domain/VP16 acidic activation domain/Gal4 DNA-binding domain; HPT, hygromycin phosphotransferase; *LacO*, 256mer of *lac* operator arrays; LB, left border; RB, right border. (b) Molecular characterization of the integrated loci with T-DNAs. The number of integrated loci was first characterized by Southern blot analyses, and the borders of the insertion sites were subsequently defined by subcloning and sequencing of the respective regions for the different sites using various strategies. The solid circle indicates the location of the centromere. The entire length of the chromosome and the distance between the two insertion loci are indicated in Mbp. Arrows indicate the direction of T-DNAs from LB to RB. Shaded rectangles represent neighboring reading frames around the T-DNA inserts.

endopolyploid cells with enlarged nuclei. Endoreduplication is widely observed in the animal and plant kingdoms, although it is more common among insects and angiosperms that have small genomes (Nagl, 1976). Constant tissue-specific patterns of endoreduplication in different organs and cell types suggest that endoreduplication is an essential part of the developmental programs in post-mitotic cells (Mizukami, 2001). In fact, ploidy levels affect gene expressions in budding yeast (Galitski et al., 1999) and plants (Lee and Chen, 2001). It was of interest to us to study the effects of endoreduplication on chromatin dynamics because it could provide clues to the mechanisms that mediate changes in gene expression in polyploid cells (Edgar and Orr-Weaver, 2001; Madlung et al., 2002).

Materials and Methods

Transgenic *Arabidopsis*

Second and fourth generation seedlings from the EL702C homozygous line (Kato and Lam, 2001) were used in this study. Seeds were germinated for 2-3 weeks in a plant growth chamber on 0.5× MS agar plates [2.1 g l^{-1} Murashige and Skoog salts (Invitrogen, CA) and 0.7% bacto-agar, pH 6.0] containing 37 mg l^{-1} of hygromycin prior to analysis.

Genomic library screening

Genomic DNA of homozygous EL702C *Arabidopsis* plant was extracted and digested with *Bgl*II and *Hin*dIII to release the T-DNA left border region from the *lac* repressor expression cassette together

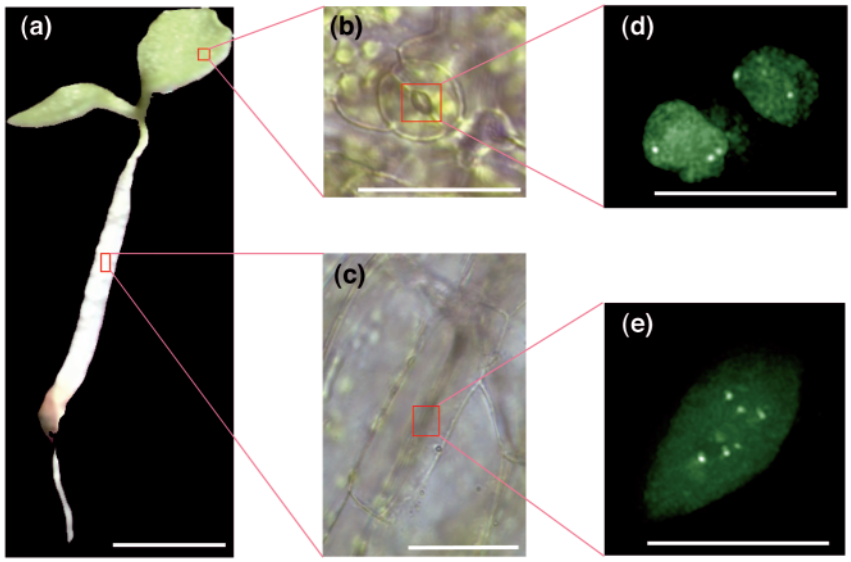

Fig. 2. Representative images of *Arabidopsis thaliana* EL702C seedling, guard cells, pavement cells and nuclei observed in this study. (a) A live seedling used to observe chromatin movements. Bar, 1 mm. (b) Microscopically observed stomatal guard cells on a cotyledon. Two guard cells symmetrically located. Bar, 50 μm. (c) Microscopically observed pavement cells on a hypocotyl. Elongated rectangular cells fill the surface of the hypocotyl. Bar, 50 μm. (d) Guard-cell nuclei accumulating GFP-LacI/NLS in two guard cells. Three spots can be seen in the left nucleus and two spots in the right nucleus. Bar, 10 μm. (e) A pavement-cell nucleus accumulating GFP-LacI/NLS. Six spots can be seen in this nucleus. The nucleus elongates to opposite sides, parallel to the long axis of the hypocotyl. Bar, 10 μm.

with genomic DNA flanking the insertion sites. DNA fragments of 2-5 kbp were used to construct the partial genomic DNA library with a ZAP Express, *Bam*HI-predigested Gigapack cloning kit (Stratagene Cloning Systems, CA). The library (2×10^5 pfu) was screened with radiolabeled T-DNA left border region DNA fragments (Kato and Lam, 2001).

Adaptor PCR screening

*Bgl*II and *Hin*dIII-digested genomic DNA fragments of 2-5 kbp were eluted from an agarose gel and ligated to a *Bam*HI cassette that is provided with the LA-PCR in vitro cloning kit (Takara, Japan). PCR was performed according to the manufacturer's protocol. Oligonucleotides (5′-ATGTCTCTGACCAGACACCCATCAACAG-TA-3′ and 5′-GGGATCCTGTACTCCACCAAAGAAGAAGAG-3′) whose sequences are present in the T-DNA left border region were used as defined region-specific primers.

Sample preparation for microscopy

Surface-sterilized seeds were germinated on 0.5× MS agar plates. 1-2-week-old seedlings were transferred to fresh 0.5× MS agar plates and 40 μl of a 0.3 μM dexamethasone (Dex) solution was then dropped on each seedling. After 10-12 hours, the seedlings were placed between two coverslips under water. The coverslips were then placed on the microscope stage for microscopic imaging.

DAPI staining

We followed the method described by Melaragno et al. (Melaragno et al., 1993). Homozygous EL702C seedlings were fixed in a solution of three parts 95% ethanol to one part glacial acetic acid for 2 hours at room temperature and then transferred to 70% ethanol. Fixed cells were then soaked in water and transferred into 0.5 M EDTA containing 5 μg ml^{-1} of 4′,6′-diamidino-2-phenylindole (DAPI) for 1 hour. The stained seedlings were washed with water and set on the microscope slides as described above. Nuclear images were obtained with a 60× water-immersion objective lens and two-dimensional non-deconvolved nuclear images were used to obtain the fluorescence intensities. The mean intensity of three nuclei in root tip cells was used to compare the relative intensities of guard cell and pavement cell nuclei. Three independent samples were used.

Fluorescence microscopy and spot detection

A DeltaVision restoration microscope system (Applied Precision, WA) equipped with a TE200 microscope (Nikon, Japam) was used to observe nuclei in Dex-induced seedlings. 40 images at 0.2 μm *z*-axis steps were collected using a Nikon PlanApo 60× 1.2 NA water-immersion objective lens. The exposure times were 0.3-3.0 seconds and the filters used were: exciter, 436 nm/10 nm; emitter, 470 nm/30 nm; and a JP4 beamsplitter (Chroma, VT). The images presented were deconvolved based on a point-spread function data.

Because a relatively high accumulation of GFP is required to visualize spots in the nucleus, the background-to-signal (free versus bound GFP fusion protein) ratio is a significant factor. High levels of GFP accumulation might also cause nonspecific GFP aggregation. Thus, the nuclei were observed under conditions with minimal GFP accumulation (6-12 hours after induction with 0.3 μM Dex) and *lac*-operator-binding GFP spots were defined statistically. In this work, the spots were defined as a cluster of pixels that contained outliers in images of the observed nuclei. The intensity values (16-bit integer) of each pixel in optically *z*-axis-sectioned images were measured and the outlier is defined as:

$$o > m + 3.3s ,$$

where *o* is the outlier, *m* is the mean of total pixels and *s* is the standard deviation from the mean. Under these conditions, the control line (transformed with a construct that does not contain *lac*-operator arrays) rarely showed any GFP spots (<2%) whereas hemizygous EL702C plants infrequently showed nonspecific GFP aggregations in a few cases (<3%) (data not shown).

Measurement of nuclear volumes

Volumes of the nuclei were estimated by measuring diffused GFP background fluorescence in the nuclei, which were used to measure chromatin movements, at the first time point. Deconvolved three-dimensional (3D) nuclear images were analysed to obtain the volumes. GFP signals were selected in each optical section and the volumes were calculated as a sum of GFP signal areas in a total of 40 sections.

Measurement of chromatin movement

Overall mean-square differences in distance between GFP spots $<\Delta d^2>$ plotted against elapsed time intervals Δt in guard-cell nuclei of cotyledons from EL702C homozygous plants are measured. When the data on the 12th (11 minutes) and 13th (12 minutes) time points were collected, the exciter shutter was closed from the 3rd to 10th points in order to minimize photobleaching of the samples.

Plants were fixed by treatment with ice-cold methanol for 5 minutes followed by ice-cold acetone for 30 seconds. The seedlings were immediately dried with paper towels and floated in a Petri dish with distilled water until it was set on the microscope slide.

Image processing

The stacked images of nuclei were analysed by softWoRx software (Applied Precision, WA) on an Octane Workstation (Silicon Graphics, CA). The images were then processed by Adobe Photoshop 5.5 (Adobe Systems, CA) on a PowerMac G4 computer (Apple, CA) for the final images.

Results

Molecular characterization of the inserted loci in transgenic *Arabidopsis* line EL702C

The number of integrated loci was characterized by Southern blot analysis, and the borders of the insertion sites were defined by sequencing respective integration sites using a genomic DNA library cloning strategy coupled with adaptor PCR. In the transgenic line designated as EL702C, we found three T-DNAs inserted into two linked loci on the upper arm of chromosome 3 with an interlocus distance of ~4.2 Mbp (Fig. 1b). The insertion closer to the top end of the chromosome appears to be a simple insertion. The single T-DNA was integrated in a non-coding region ~1.6 Mbp away from the top end of the chromosome. A gene that encodes an unclassified protein, the 26S proteasome AAA-ATPase subunit RPT5a [*Arabidopsis* Genome Initiative (AGI) annotation number: AT3g05520] is located 0.4 kbp from the left border (LB) of this T-DNA insert. The other neighboring gene, which encodes an unclassified protein [the α subunit of F-actin capping protein (AGI number: AT3g05530)], is located 2.0 kbp from the right border (RB) of this insert. The other two T-DNA inserts were inversely integrated in the same locus with a predicted 15 bp gap. An unidentified reading frame (URF) (AGI: AT3g16880) is disrupted by the inserts. One URF (AGI: AT3g16870) is located 1.9 kbp upstream of the LB for the insert, closer to the top of the chromosome arm, and another URF (AGI: AT3g16890) is located 0.7 kbp from the LB of the distal insert. Owing to the close proximity of these two inserts, we treat them as a single locus in our interpretation of microscopy

observation in addition to the other single insertion, 4.2 Mbp away.

Comparative analysis of nuclear properties for guard cells and pavement cells in homozygous EL702C seedlings

In *Arabidopsis thaliana*, ploidy levels for cells can vary from 2C (stomatal guard cells, sepal and petal epidermal cells) to 64C (leaf trichome) (Melaragno et al., 1993). Guard cells are components of stomata that regulate gas exchange and are distributed across the leaf and hypocotyl epidermis with characteristic spacing. These cells develop in pairs symmetrically from common mother cells and their cell cycle is arrested in G1 phase after differentiation (Melaragno et al., 1993). The shape of the differentiated cell is a uniformed crescent shape (Fig. 2b), whereas their nucleus is usually disk-like (Fig. 2d). In contrast to guard cells, pavement cells fill the surface of hypocotyl epidermis and grow in one direction without cell division, resulting in elongated, rectangular shapes (Fig. 2c). These cells contain a large nucleus that is usually elongated along the axis of the hypocotyl, and mature pavement cells have typically undergone several rounds of endoreduplication (Fig. 2e).

We first characterized the nuclei of guard cells and pavement cells in homozygous EL702C seedlings by fluorescence microscopy after Dex induction. In guard-cell nuclei, the spot numbers observed upon Dex treatment vary from none (not detected) to four (Fig. 2d, Fig. 3a); ~40% of the guard cells in homozygous lines showed two spots. In pavement cell nuclei, the spot numbers were more variable and ~10% of cells showed up to eight spots (Fig. 2e, Fig. 3a).

To verify the expected ploidy difference between guard cells and pavement cells, the relative quantities of DNA in nuclei of these two cell types were measured by DNA-specific DAPI staining. Fluorescent intensities of each nucleus were compared with the average intensities of root-tip-cell nuclei, in which the ploidy level is known to be 2C (Melaragno et al., 1993). Fluorescent intensities of guard-cell nuclei in the homozygous EL702C line are the same as root-tip-cell nuclei (Fig. 3b). By contrast, DAPI fluorescence intensities in pavement cell nuclei are two to eight times higher than root-tip cells, and the average intensity is approximately five times higher than that of guard cells (Fig. 3b). These results are consistent with previous studies (Melaragno et al., 1993). The difference in nuclear volumes between guard cells and pavement cells was determined by calculating the volume of diffuse GFP background fluorescence caused by unbound fusion proteins in 3D models of the nuclei (Kato and Lam, 2001). In guard cells, nuclear volumes are ~50 μm^3, whereas the volumes of nuclei in pavement cells are ~250 μm^3 on average (Fig. 3c). The positive relationship between nuclear volume and ploidy levels is consistent with previous findings (Baluska, 1990) and shows that the guard cells and the pavement cells we observed display the expected degree of ploidy. In this study, we did not measure the GFP spot numbers in the same samples that were used for DAPI staining because DAPI staining affected GFP-LacI/NLS induction and might also affect the viability of the samples. Therefore, we could not directly address the relationship between GFP spot numbers and ploidy level within the same nuclei.

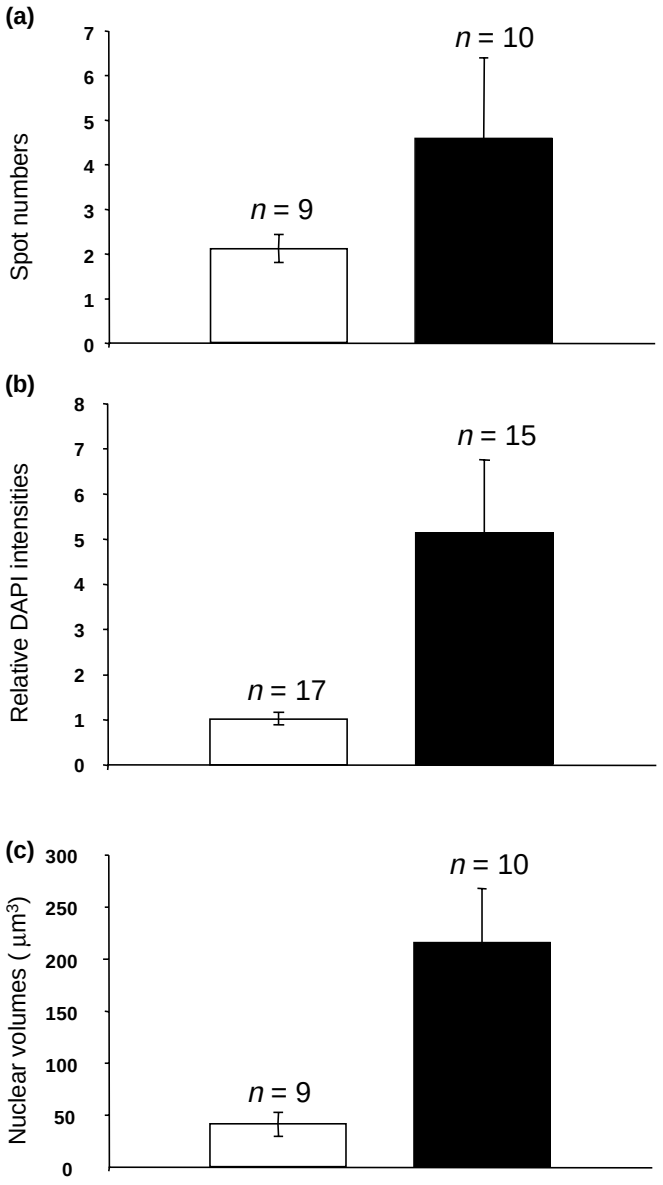

Fig. 3. Nuclear properties of guard cells and pavement cells in homozygous EL702C seedlings. (a) GFP spot numbers observed in guard-cell nuclei (open column) and in pavement-cell nuclei (closed column). Spot numbers were counted in a total of nine guard-cell nuclei and ten pavement-cell nuclei whose chromatin movements were measured. The mean spot numbers per nucleus are shown with the standard deviations from the mean indicated. The number of samples analysed is indicated by '*n*' on the graph. (b) Relative nuclear DNA contents of guard-cell nuclei (open column) and pavement-cell nuclei (closed column). The samples were stained with DAPI and the nuclear intensities in guard cells (total of 17 in three seedlings) and pavement cells (total of 15 in three seedlings) were compared with that in root-tip cells (whose ploidy is known to be 2C). The mean relative intensities are shown with the standard deviations from the mean. The number of samples analysed is indicated by '*n*' on the graph. (c) Nuclear volumes in guard-cell nuclei (open column) and pavement-cell nuclei (closed column). The nuclear volumes in a total of nine guard-cell nuclei and ten pavement-cell nuclei whose chromatin movements were measured were calculated by measuring the non-*lac*-operator-binding GFP signals in nuclei. The mean volumes per nucleus are shown with the standard deviations from the mean indicated. The number of samples analysed is indicated by '*n*' on the graph.

Chromatin dynamics in guard cells and pavement cells

To compare chromatin dynamics in diploid and endoreduplicated nuclei, we characterized the motion of the inserted loci in nuclei of guard cells and pavement cells in live EL702C *Arabidopsis* seedlings after Dex induction. Chromatin motions were represented by plotting the overall mean squared change in distance $<\Delta d^2>$ between two spots against elapsed time interval Δt (Marshall et al., 1997b). For two freely diffusing objects undergoing random-walk motion, a plot of $<\Delta d^2>$ against Δt should increase continuously if the movement is not constrained. If the movement is constrained to a certain area, $<\Delta d^2>$ should become independent of Δt over time and the plot will plateau.

First, we measured the chromatin movement in guard cells. We detected two spots in most of the analysed nuclei. We measured the distance between pairs of spots per nucleus as a function of time. As a total, we measured nine pairs of spots in a total of nine nuclei. The plot of measurements taken from live plants produced $<\Delta d^2>$ values that essentially remain unchanged in the range of 10 minutes (Fig. 4). We compared the plot to that observed with chemically fixed plants and found that the value of $<\Delta d^2>$ for live cells showed an approximately three times higher range at all time points measured, demonstrating that the movements are not due to experimental error or instrument noise. The asymptotic $<\Delta d^2>$ value of 0.03 μm^2 (Fig. 4) indicates a mean change in distance between two spots of 0.17 μm. The maximum radius of the constrained area for guard cell nuclei, which was obtained by measuring Δd for various time points from independent experiments (data not shown) was 0.21 μm. The results indicate that the tagged loci in the transgenic line undergo diffusive movement in constrained areas within the nucleus. For particles undergoing 3D random walks with a diffusion constant D, it can be shown that a plot of $<\Delta d^2>$ against Δt should increase linearly with a slope of 4D (Marshall et al., 1997b). Thus, one can estimate the diffusion constant based on the plots. In *Drosophila* spermatocytes, diffusion coefficients of early G2 phase chromatin are 1.0×10^{-3} μm^2 s^{-1} and 0.94×10^{-4} μm^2 s^{-1} in late G2 phase. At the present time, with our experimental system, it takes ~50 seconds to detect the tagged loci with high signal-to-noise ratios using 3D restoration microscopy. Thus, we are unable to perform more rapid time-lapse measurements of the relative distance between two tagged loci. We consequently could not measure precisely the earlier phase in the plot of $<\Delta d^2>$ versus Δt in order accurately to determine the precise diffusion coefficient for individual tagged loci. However, because the asymptotic value of $<\Delta d^2>$ (0.03 μm^2) was apparently reached in less than 1 minute, we estimate this would put a lower limit of 1.25×10^{-4} μm^2 s^{-1} for D, assuming that the plot of $<\Delta d^2>$ against Δt reaches a plateau at 1 minute in a linear fashion.

Next, we measured the chromatin movement of pavement cell nuclei by a plot of the overall mean squared change in distance $<\Delta d^2>$ between two spots for the elapsed time interval Δt (Fig. 4). The spot numbers varied between three and six spots in analysed nuclei. In most cases, 'spot numbers – 1' pairs were measured for each of the nuclei studied. As a total, we measured 36 pairs of distances in ten nuclei. We also performed similar measurements with pavement cell nuclei that were chemically fixed to confirm that the different movements from guard cell nuclei are not caused by altered conditions when dealing with different cell types in different parts of the plant. Plots of measurements made with pavement cell nuclei show that $<\Delta d^2>$ increases until 7 minutes (Δt) and reached a plateau of 0.10 μm^2, which indicates a mean change in distance between the spots of 0.32 μm. The maximum radius of the confinement area, which was also obtained by measuring Δd for various time points from independent experiments (data not shown), was 0.44 μm. Diffusion coefficients calculated from the slope is 5.35×10^{-5} μm^2 s^{-1}. We did not detect any correlation for distances between the pairs of spots and the changes (i.e. there is no evidence that spots close to each other move less than spots that are further apart) in this work.

The Student's *t*-test for $<\Delta d^2>$ values using a two-tailed distribution between the samples of diploid guard cells and endoreduplicated pavement cells at 9 minutes and 10 minutes gave *P* values of 0.0050 and 0.0054, respectively. This suggested that the values of $<\Delta d^2>$ at the plateau are significantly different. Our results indicate that chromatin movement of endoreduplicated pavement cell nuclei might

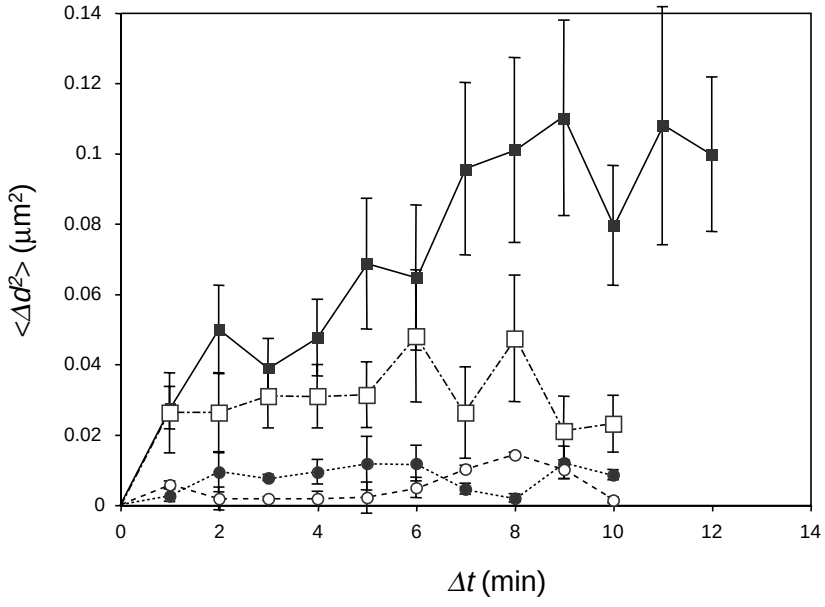

Fig. 4. Chromatin dynamics in guard-cell and pavement-cell nuclei. Overall mean-square differences in distance between GFP spots $<\Delta d^2>$ plotted against elapsed time intervals $<\Delta t>$ in guard-cell (□) and pavement-cell (■) nuclei of homozygous EL702C seedlings. Each data point represents an average of data collected from at least nine independent experiments. Open circles (○, guard-cell nuclei) and closed circles (●, pavement-cell nuclei) represent data from fixed seedlings, which were imaged under identical conditions with data points representing averaged values from at least six independent experiments and nine nuclear observations. Vertical bars at each time point show the standard errors for the particular set of data collected. If the motion were not restricted, $<\Delta d^2>$ would continue to increase with increasing time. The longer the time interval between measurements, the greater the distance between two diffusion points is expected to change.

have a lower diffusion coefficient (<2.3 times) but larger constrained areas (6.6 times larger on average and 9.2 times as a maximum) than guard cell nuclei.

Discussion

Variance of GFP spot numbers in the observed nuclei

The GFP spot numbers in the observed nuclei varied from measurement to measurement. This suggests that some of the tagged loci might associate stochastically with each other, in a manner similar to a previously reported phenomenon in budding yeast (Aragon-Alcaide and Strunnikov, 2000). We tested whether spot size or fluorescence intensity is correlated with the spot numbers but we could not find positive correlations in either guard cells and pavement cells (data not shown). This could be due to differences of spot positions in the *z*-axis. Meanwhile, we found that the rate of association in pavement cells is higher than that in guard cells. We do not yet know whether the higher rate of association in the pavement cells is caused by the stochastic association of the insertion loci or whether each replicated chromatid remains cohered in nuclei that undergo endoreduplication.

However, we can estimate the coherence probabilities of multiple chromatids in endoreduplicated cells by comparing the average GFP spot numbers and the average DAPI fluorescence intensities in endoreduplicated pavement cells versus diploid guard cells. If all chromatids are separated, the ratio of GFP spot numbers in pavement cells to guard cells would be the same as that for DAPI fluorescence intensities. By contrast, if all chromatids remain cohered, the GFP spot numbers would not increase (guard-cell to pavement-cell ratio of 1). Because the increment of GFP spot number ratio (2.5 times on average) is half of that for the increase in DAPI fluorescence intensities (five times on average) in this study (Fig. 3a,b), we predict that half of the chromatids might remain cohered while the other half are separated in the endoreduplicated pavement cells. This is consistent with the recent fluorescence in situ hybridization (FISH) observation using fixed 4C nuclei with single-locus probes for chromosome 4. The observation suggests that ~50% of the chromatids in endoreduplicated nuclei are not cohered (M. Klatte, V. Schubert and I. Schubert, personal communication).

Chromatin attachment in plant interphase nuclei

In both guard cells and pavement cells, chromatin shows constrained diffusion movement (Fig. 4). This suggests that plant chromatin is tethered by static interactions within nuclei, as found in other organisms (Chubb et al., 2002; Heun et al., 2001; Ishii et al., 2002). The result allows studies of chromatin dynamics, which have been done in yeast and animals, to be extended to plants with regards to the mechanism of interchromosomal interactions. Lamin proteins are thought to provide scaffolding structures that mediate the attachment of chromatin to the nuclear envelope in animal cells (Gant et al., 1999; Lopez-Soler et al., 2001). However, lamins have not been identified in plants or the budding yeast *Saccharomyces cerevisiae* (Meier, 2001). This fact and our present finding suggest that plants and yeast might have a distinct set of nuclear anchoring components that functionally replace lamins of animal cells.

Factors that increase chromatin constrain areas in endoreduplicated pavement cells

One of the features of endoreduplicated nuclei is increase in nuclear volume (Baluska, 1990). Although the biological consequences of the enlarged nucleus on nuclear processes such as transcription are not clear (Edgar and Orr-Weaver, 2001), a simple explanation of this feature is that nuclear volume is proportional to ploidy levels to maintain a similar 3D space per haploid genome. The measured increase in nuclear volume in pavement cells is approximately the same as the estimated increase in DNA content relative to diploid guard cells (Fig. 3b,c). Moreover, half of the chromatids in endoreduplicated pavement cells are thought to be separated, as discussed above. These features suggest that pavement-cell nuclei indeed contain a similar (twofold difference in maximum) 3D space per haploid genome as guard-cell nuclei.

By contrast, we found that the apparent confinement areas for chromatin movement of endoreduplicated pavement-cell nuclei are over six times larger than those found in guard-cell nuclei. This finding suggests that the chromatin in endoreduplicated pavement cells has larger free spaces of diffusion than that in guard-cell nuclei even though the chromosome space per haploid genome is similar. What makes the confinement areas larger in pavement nuclei than in guard cells? One simple explanation could be a reduction in the concentration of proteins involved in chromatin organization in the larger pavement-cell nuclei. This might result in an enlarged free space for chromosome motion in these endoreduplicated cells, because of a decrease in the number of anchoring sites or interactions for chromatin within the nucleus. In fact, daughter nuclei of early G1 phase yeast cells, which are 40% smaller than the mother-cell nuclei, show five-times-less-frequent large rapid chromatin movements than mother cells in the same culture (Heun et al., 2001).

Another observation that lends support to this explanation is the fact that endoreduplicated cells of maize root show a decrease in staining with Fast Green FCF, which stains basic proteins within the nuclei (Balusuka and Kubica, 1992). An alternative explanation is that the compositions of the chromatin-organizing proteins are different between the two types of nuclei. Although the functional significance of matrix-attachment motifs in both *cis*- and *trans*-acting elements remains unclear, the importance of structural features of *cis*-acting elements such as a narrow minor groove in A/T-rich DNA has been suggested (Kas et al., 1989). It can be hypothesized that endoreduplicated nuclei have a different type or sets of chromatin-organizing proteins from diploid nuclei. Their different sequence affinity for anchoring chromatin and changes in their quantities or composition could result in alteration of chromatin dynamics. Therefore, it would be interesting to determine whether diploid and endoreduplicated nuclei have different biochemical compositions in matrix proteins.

Biological significance of increased confinement areas in pavement cells

Changes of gene expression associated with ploidy differences in budding yeast is not caused by alterations in growth rate or viability but instead by an increase of DNA content (Galitski et al., 1999). Allotetraploid (hybrid genome)-dependent

changes in gene expression of *Arabidopsis* have also been reported (Lee and Chen, 2001). In the study, genes silenced in *Arabidopsis suecica*, an allotetraploid derived from *Arabidopsis thaliana* and *Cardaminopsis arenosa*, were investigated with an amplified fragment-length polymorphism (AFLP) cDNA display method. The result indicates epigenetic regulation of orthologous genes in polyploid genomes.

Epigenetic mechanisms can involve interchromosomal interactions. For example, paramutation can silence allelic genes in heterozygous conditions (Sidorenko and Peterson, 2001) whereas transvection can change gene expression by combining an enhancer on one chromosome and a promoter on another chromosome (Wu and Morris, 1999). Marshall explained the relationship between interchomosmal interactions and chromatin diffusion confinement as follows (Marshall, 2002). If two loci are to interact physically, they must be located within the same 3D space in the nucleus. However, because of non-random nuclear organization, not every pair of loci will be equally likely to interact. Owing to constrained diffusion, only those loci whose regions of confinement overlap are capable of interacting; pairs of loci whose confinement regions do not overlap are unable to interact because they cannot diffuse into contact.

Based on this functional model, we propose a model of developmental control of gene expression in endoreduplicated cells: although the volume of endoreduplicated nucleus is larger than that of diploid nucleus, the nuclear space per haploid genome or chromosome territories stays similar. Therefore, locus densities per nuclear space would be similar to those in diploid nuclei. Endoreduplicated nuclei allow additional or reduced intra- and interchromatin interactions by providing larger free spaces for chromatin diffusion. The expansion in the effective confinement area in the same 3D space per haploid genome (compared with the diploid nucleus) might arise from a decrease in the concentration or a change in the properties of nuclear structural proteins. In this manner, endoreduplicated cells might achieve a different gene expression pattern from diploid cells through an epigenetic mechanism. This model might also apply to the evolutionary strategy for species that carry small genomes to modulate gene expression patterns in specific cell types, which has been achieved in other species by varying DNA contents (Nagl, 1976).

This work is supported by a grant from the Plant Genome Research Program of NSF (#0077617) to E.L. We would like to thank W. Marshall for constructive suggestions on the analysis of chromosome movements and useful comments, M. Lawton for careful reading and correction of the manuscript, and N.-H. Chua for the pTA7002 vector used to construct the EL702 vector.

References

Aragon-Alcaide, L. and Strunnikov, A. V. (2000). Functional dissection of in vivo interchromosome association in *Saccharomyces cerevisiae*. *Nat. Cell Biol.* **2**, 812-818.

Baluska, F. (1990). Nuclear size, DNA content, and chromatin condensation are different in individual tissues of the maize root apex. *Protoplasma* **158**, 1-2.

Balusuka, F. and Kubica, S. (1992). Relationships between the content of basic nuclear proteins, chromatin structure, rDNA transcription and cell size in different tissues of the maize root apex. *J. Exp. Bot.* **43**, 991-996.

Chubb, J. R., Boyle, S., Perry, P. and Bickmore, W. A. (2002). Chromatin motion is constrained by association with nuclear compartments in human cells. *Curr. Biol*. **12**, 439-445.

Cremer, T. and Cremer, C. (2001). Chromosome territories, nuclear architecture and gene regulation in mammalian cells. *Nat. Rev. Genet.* **2**, 292-301.

Edgar, B. A. and Orr-Weaver, T. L. (2001). Endoreplication cell cycles: more for less. *Cell* **105**, 297-306.

Fransz, P., de Jong, J. H., Lysak, M., Castiglione, M. R. and Schubert, I. (2002). Interphase chromosomes in *Arabidopsis* are organized as well defined chromocenters from which euchromatin loops emanate. *Proc. Natl. Acad. Sci. USA* **99**, 14584-14589.

Galitski, T., Saldanha, A. J., Styles, C. A., Lander, E. S. and Fink, G. R. (1999). Ploidy regulation of gene expression. *Science* **285**, 251-254.

Gant, T. M., Harris, C. A. and Wilson, K. L. (1999). Roles of LAP2 proteins in nuclear assembly and DNA replication: truncated LAP2 beta proteins alter lamina assembly, envelope formation, nuclear size, and DNA replication efficiency in *Xenopus laevis* extracts. *J. Cell Biol.* **144**, 1083-1096.

Heun, P., Laroche, T., Shimada, K., Furrer, P. and Gasser, S. M. (2001). Chromosome dynamics in the yeast interphase nucleus. *Science* **294**, 2181-2186.

Ishii, K., Arib, G., Lin, C., van Houwe, G. and Laemmli, U. K. (2002). Chromatin boundaries in budding yeast: the nuclear pore connection. *Cell* **109**, 551-562.

Kas, E., Izaurralde, E. and Laemmli, U. K. (1989). Specific inhibition of DNA binding to nuclear scaffolds and histone H1 by distamycin. The role of oligo(dA).oligo(dT) tracts. *J. Mol. Biol.* **210**, 587-599.

Kato, N. and Lam, E. (2001). Detection of chromosomes tagged with green fluorescent protein in live *Arabidopsis thaliana* plants. *Genome Biol.* **2**, research0045.1-research0045.10.

Lee, H. S. and Chen, Z. J. (2001). Protein-coding genes are epigenetically regulated in *Arabidopsis* polyploids. *Proc. Natl. Acad. Sci. USA* **98**, 6753-6758.

Lopez-Soler, R. I., Moir, R. D., Spann, T. P., Stick, R. and Goldman, R. D. (2001). A role for nuclear lamins in nuclear envelope assembly. *J. Cell Biol.* **154**, 61-70.

Lysak, M. A., Fransz, P. F., Ali, H. B. and Schubert, I. (2001). Chromosome painting in *Arabidopsis thaliana*. *Plant J.* **28**, 689-697.

Madlung, A., Masuelli, R. W., Watson, B., Reynolds, S. H., Davison, J. and Comai, L. (2002). Remodeling of DNA methylation and phenotypic and transcriptional changes in synthetic *Arabidopsis* allotetraploids. *Plant Physiol.* **129**, 733-746.

Marshall, W. F. (2002). Order and disorder in the nucleus. *Curr. Biol.* **12**, R185-R192.

Marshall, W. F., Straight, A., Marko, J. F., Swedlow, J., Dernburg, A., Belmont, A., Murray, A. W., Agard, D. A. and Sedat, J. W. (1997a). Interphase chromosomes undergo constrained diffusional motion in living cells. *Curr. Biol*. **7**, 930-939.

Marshall, W. F., Straight, A., Marko, J. F., Swedlow, J., Dernburg, A., Belmont, A., Murray, A. W., Agard, D. A. and Sedat, J. W. (1997b). Interphase chromosomes undergo constrained diffusional motion in living cells. *Curr. Biol*. **7**, 930-939.

Meier, I. (2001). The plant nuclear envelope. *Cell Mol. Life Sci.* **58**, 1774-1780.

Melaragno, J. E., Mehrotra, B. and Coleman, A. W. (1993). Relationship between endopolyploidy and cell size in epidermal tissue of *Arabidopsis*. *Plant Cell* **5**, 1661-1668.

Mizukami, Y. (2001). A matter of size: developmental control of organ size in plants. *Curr. Opin. Plant Biol.* **4**, 533-539.

Nagl, W. (1976). DNA endoreduplication and polyteny understood as evolutionary strategies. *Nature* **261**, 614-615.

Sidorenko, L. V. and Peterson, T. (2001). Transgene-induced silencing identifies sequences involved in the establishment of paramutation of the maize *p1* gene. *Plant Cell* **13**, 319-335.

Vazquez, J., Belmont, A. S. and Sedat, J. W. (2001). Multiple regimes of constrained chromosome motion are regulated in the interphase *Drosophila* nucleus. *Curr. Biol.* **11**, 1227-1239.

Wu, C. T. and Morris, J. R. (1999). Transvection and other homology effects. *Curr. Opin. Genet. Dev*. **9**, 237-246.